

# Activation Analysis of Large Samples

**Peter Bode**

*Delft University of Technology, Delft,  
The Netherlands*

<b>1 Introduction</b>	<b>1</b>
<b>2 Large Sample Activation Analysis</b>	<b>2</b>
2.1 Large Sample Neutron Activation Analysis	2
2.2 Large Sample Prompt $\gamma$ -Activation Analysis	3
2.3 Large Sample Photon Activation Analysis	4
<b>3 Measurement Equation of Large Sample Neutron Activation Analysis</b>	<b>4</b>
<b>4 Instrumentation</b>	<b>5</b>
4.1 Neutron Sources for Large Sample Activation Analysis	5
4.2 Irradiation Facility	6
4.3 Sample Containers for Irradiation	7
4.4 Counting Facility	8
<b>5 Calibration</b>	<b>10</b>
5.1 Absolute Method	10
5.2 The Comparator Method	11
5.3 Single Comparator Method	11
5.4 $k_0$ -Based Method for Standardization	11
5.5 Internal Monostandard Method	12
5.6 Neutron Fluence Rate Monitoring	12
5.7 $\gamma$ -Ray Self-Attenuation	13
5.8 Extreme Inhomogeneities	13
<b>6 Quality Control</b>	<b>14</b>
6.1 Quality Control in Large Sample Analysis	15
<b>7 Sensitivity</b>	<b>17</b>
7.1 Natural Background	18
<b>8 Applications</b>	<b>18</b>
8.1 Materials Difficult to Homogenize: Geological Samples, Ores, and Waste	18
8.2 Materials That May be Contaminated During Homogenization: High-Purity Materials	19
8.3 Materials Difficult to Subsample: Nutritional Studies	19
8.4 Valuable Material of Irregular Shape	19

8.5 Other Applications	19
<b>References</b>	<b>19</b>

*There is a trend in many analytical techniques towards the use of smaller sizes of the test portion, and sometimes submilligram amounts are being used. The limitation to the size of the test portion can pose the analyst with problems when the amount of material collected is large. Subsampling and preparation of a representative test portion may be difficult if homogenization is impossible or extremely expensive, or if homogenization introduces contamination. An alternative approach has been introduced in the 1990s by the development of large sample neutron activation analysis (LSNAA), later followed by large sample photon activation analysis. These techniques are capable of direct analysis of samples with masses of hundreds of grams to several kilograms. Though the principles and physics of large sample activation analysis are thoroughly understood, the method is still not as versatile or applicable as, for example, normal small sample neutron activation analysis. In this article, the physics of LSNAA is described, including methods of calibration. Examples are given of irradiation and counting facilities and the special aspects of quality control are discussed. Several examples are given of applications of large sample analysis, e.g., for studies related to electronic waste, complete archaeological and cultural artifacts, high-purity materials, and materials of irregular shape.*

## 1 INTRODUCTION

All the routine multielemental analysis techniques (inductively coupled plasma atomic emission spectrometry (ICP-AES), inductively coupled plasma mass spectrometry (ICP-MS), and instrumental neutron activation analysis (INAA), etc.) employ rather small test portions of material, varying from a few milligrams to a few grams of solids or in the range of a few milliliters in the case of liquids<sup>(1)</sup> (see Table 1). There is even a tendency to go for smaller test portions, such as in solid-state atomic absorption spectrometry (AAS), laser-ablation ICP, and total reflection X-ray fluorescence (XRF) spectrometry. In XRF, the use of quantities larger than required to prepare the target is anyhow meaningless, as the derived information is from the surface layers, representing a few milligrams only.

The limitation to the size of the test portion can pose problems to the analyst when the amount of material collected is large. This is often the case since soils, rocks, plant material, etc. can be more easily and

**Table 1** Sizes of the samples and analytical portions handled in several multielement analysis techniques<sup>(1)</sup>

Analysis technique		Solid material mass used or prepared to test portion	Volume used as test portion
Atomic absorption spectroscopy (AAS)	Gas furnace	Typically 1–2 g dissolved; maximum approximately 10 g	10–20 $\mu$ L
AAS	Flame		1–2 mL
Inductively coupled plasma spectroscopy (ICP)		Typically 1–2 g dissolved; maximum approximately 10 g	Approximately 500 $\mu$ L
X-ray fluorescence spectroscopy (XRF)		10 g	
Instrumental neutron activation analysis (INAA)		Typically approximately up to 500 mg; in some cases up to 30 g	1–50 mL

representatively sampled at quantities in the order of hundreds of grams to kilograms than at quantities less than 1 g. A sample is denoted as “representative” when “it can be expected to exhibit the average properties of the material, environment or population it was taken from”.<sup>(2)</sup> Representativeness is a priori preserved when (i) the sampling is performed according to specific, certified norms or when (ii) a truly homogeneous material is sampled. Homogeneity is defined as “the degree to which a property or substance is randomly distributed throughout the material”.<sup>(2)</sup>

Homogeneity depends on the size of the units under consideration. A mixture of minerals may be inhomogeneous at the molecular or atomic level but homogenous at the particle level. In chemical analysis this unit is obviously correlated with its effect in the conduct of the analysis (e.g. differences in solubility) or in its interpretation. Thus, both from practical and sampling considerations often more material is collected and presented for analysis than can be handled.

Irrespective of the analysis technique selected, attention has to be paid to representative subsampling to obtain a relevant final analytical portion from the originally collected material. When restricting the discussion to the analysis of solid materials, this subsampling may imply sample size reduction techniques and other processing such as sieving, crushing, milling, or blending. Problems of the following types arise:

1. Homogenization is impossible, or extremely expensive, because of material properties. Examples are electronic circuits on printed boards, household waste, and scrap from recycled electronics, automobiles, and plastics. A solution to this problem is to sort the material and to perform individual homogenizations and, subsequently, analyze, thereby increasing the total project costs.
2. The homogenization step results in contamination of the sample. Often the contamination due to crushing or milling is not controllable on every sample type. When processing a large series of samples, careful

interim cleaning may get less attention since it is time consuming and therefore expensive.

Testing the degree of homogeneity is a common practice in the preparation of reference materials, but for routine operations, such a procedure, the requirement of analysis and statistical evaluation of at least five or more test portions of each sample, would raise the cost of the analysis considerably.

Considerations from the above indicate that direct analysis of the voluminous solid sample as collected might have advantages, both analytical and economical.

Detection limits in trace-element studies are based on the signal-to-noise ratio. An additional feature of analysis of large test portions is that the detection limit for trace elements may be decreased considerably in case of high-purity materials. This was demonstrated, for example, by Verheijke<sup>(3)</sup> in the assessment of impurities in (5 in. diameter) silicon wafers to be used in the electronic industry.

## 2 LARGE SAMPLE ACTIVATION ANALYSIS

### 2.1 Large Sample Neutron Activation Analysis

In analytical terms, a “large sample” can be anything exceeding the regular size of a test portion in the process to determine the components of the material. The regular mass of a test portion in neutron activation analysis (NAA) varies from a few milligrams to 1 g. As already indicated, instrumental neutron activation analysis (INAA) has all the potentials to analyze, with adequate accuracy, test portions<sup>(4)</sup> in the kilogram range.<sup>(5–8)</sup> Both the incoming radiation for activation (neutrons) and the outgoing radiation to be measured ( $\gamma$ -rays) have sufficiently high penetrating power to facilitate NAA of portions of samples weighing kilograms. A “large sample” in NAA is defined as a test portion in which neutron and  $\gamma$ -ray self-attenuation cannot be neglected in view of the required degree of accuracy.

A few phenomena need more attention in large sample neutron activation analysis (LSNAA) than in normal NAA (handling test portions varying from micrograms to a maximum of 0.5 g), where these phenomena usually have only insignificant impact to the degree of accuracy of the results.<sup>(9)</sup> In large test portions, e.g., of kilogram size, neutron absorption and scattering result in substantial self-shielding, causing depression of the neutron flux at the center of the sample compared to the periphery. Neutron self-thermalization may cause substantial changes in the neutron spectrum throughout the sample if the sample material also contains, for example, hydrogen.

Similarly, the  $\gamma$ -radiation of the activation products deep inside in the sample will be more strongly absorbed and scattered before leaving the sample than the radiation resulting from, e.g., the surface of the sample; moreover the absorption and scattering increase rapidly at lower  $\gamma$ -ray energies. This effect is denoted as  *$\gamma$ -ray self-attenuation*. In addition, a sample of, say, 1 kg cannot be considered anymore as a more-or-less “point source” during counting at normal sample–detector distances of, e.g., 10–30 cm, resulting in a corresponding different response of the detector for the  $\gamma$ -radiation. In contrast to conventional INAA with small samples, analysis of test portions larger than a few hundred milligrams requires correction for these neutron self-shielding and  $\gamma$ -ray self-absorption effects, either via calibration or by modeling.

Trace-element determinations in large test portions have been carried out for decades in areas such as well logging,<sup>(10)</sup> on-line conveyor belt industrial analyzers,<sup>(11)</sup> and in vivo studies of, e.g., Ca in bones and Cd in kidneys.<sup>(12)</sup> In all these studies, the NAA technique is applied since the strong penetration of the neutrons as well as the resulting emitted  $\gamma$ -radiation (either prompt during the nuclear reaction or delayed from the activation products) allows bulk analysis rather than surface analysis, the “limiting” factor in XRF spectrometry. For cases such as coal and ore analysis, these bulk analyses have been applied in industrial settings and for field-mineral explorations using 14 MeV neutron generators<sup>(13)</sup> and isotopic neutron sources.<sup>(14)</sup> The analyses are mainly focused on raw material analysis and for product control of one or a few major constituents. These procedures are, through calibration, customized for the problems they have been developed for and cannot be translated into a routinely applicable method for the analysis of a large variety of sample types. The same applies to the use of NAA principles in well-logging devices, in which the entire surrounding rock may be considered as a large sample.

The advantage of reactor-based INAA in the analysis of large samples lies with the higher available neutron fluxes and activation cross sections, all leading to better

sensitivities for trace elements than can be obtained with 14 MeV neutron generators and isotopic neutron sources and providing the opportunity for full multielement analysis.

LSNAA has evolved over the years<sup>(15–20)</sup> toward a capability for analysis of various samples types which otherwise would have been difficult to analyze. Both off-line (LSNAA) and on-line (LS-prompt  $\gamma$ -NAA) activation methods are used. The emphasis in this article is on (off-line) LSNAA; prompt  $\gamma$ -LSNAA is discussed briefly below.

## 2.2 Large Sample Prompt $\gamma$ -Activation Analysis

Large sample prompt  $\gamma$ -neutron activation analysis (PGNAA) is being applied for many years in well logging, industrial (conveyor) belt analyzers, etc. using isotopic neutron sources such as <sup>252</sup>Cf or <sup>241</sup>Am(Be). The advantage of isotopic source-based PGNAA compared to normal NAA lies in the fact that the test portion may be analyzed locally rather than having to be taken to the laboratory and on-line information is obtained. Since the output of the sources is rather low, large samples are needed anyhow to obtain a measurable signal, usually from the main components in the material of interest. Industrial analyzers are commercially available for the on-line analysis of cement,<sup>(21)</sup> the determination of the sulfur content on coal,<sup>(22)</sup> for the detection of explosives in airline cargo,<sup>(23)</sup> etc.

Reactor-based large sample PGNAA, i.e. using an external neutron beam, was demonstrated by Sueki et al.<sup>(24)</sup> for a pottery sample of 15 cm diameter, 10 cm width, and 0.5 cm wall thicknesses. The neutron beam dimensions were approximately 2 cm  $\times$  2 cm.

Similar to “normal” LSNAA, in large sample PGNAA also the problems of neutron attenuation and  $\gamma$ -ray self-shielding have to be solved. In the example quoted above, the internal monostandard was used (see Section 5.3). Also, other intact archaeological objects were analyzed by this method, such as bronzes.<sup>(25)</sup> Moreover, neutron beams from reactors are relatively limited in dimensions (on the order of 5 cm  $\times$  3 cm), which sets also a limit to the size of the object activated. This limitation can be overcome by repositioning the sample in the beam.

An advantage of large sample PGNAA over normal LSNAA is that no special facilities have to be constructed in the reactor, and that the sample contains hardly any induced radioactivity, which is of importance when dealing with, for example, archaeological or cultural artifacts. The PGNAA setup can be standard,<sup>(24)</sup> but care has to be taken that the large object does not “transform” into a very intense source of prompt  $\gamma$ -radiation with associated radiation dose hazards for the researchers.

Other methods for standardization have been proposed too, and mostly are based on a priori available information on the (gross) composition of the object; e.g. using Monte Carlo simulations<sup>(26)</sup> or neutron transport codes<sup>(27)</sup> (“fixed point iteration method”). Degenaar developed a method in which no a priori information is used and the neutron self-shielding is estimated on basis of the attenuation and scattering of the neutron beam, measured outside the sample.<sup>(28)</sup>

### 2.3 Large Sample Photon Activation Analysis

Photon activation analysis has the potential to analyze very large samples for reasons similar to NAA: large penetration power of the incident bremsstrahlung photons (typically in the order of several tens of million electronvolts), and similar to NAA, large penetration of the  $\gamma$ -radiation from the induced radioactivity. There is also some similarity to prompt  $\gamma$ -NAA with respect to the size of the object that can be exposed at a time; here also, the sample can be “moved” through the beam to attain a homogeneous activation, or the beam can be scanned over the sample. It introduces an additional complication if the integral sample is counted after exposure: the different activated parts have different decay times but their signals are registered simultaneously. Alternatively, one may choose to limit the sample size.

At the Bundesanstalt für Materialprüfung (BAM) in Berlin, Germany, large sample photon activation analysis has been applied<sup>(29)</sup> using the 30 MeV linear accelerator for studies involving samples with sizes in the order of 8 cm height and approximately 2 cm thickness with masses of up to 100–200 g. The measurements were done using a twin detector set up; i.e. the sample was “sandwiched” between two side-looking semiconductor detectors.

One of the advantages of photon activation analysis over NAA is that the corrections for self-attenuation of the incoming bremsstrahlung photons are relatively easy to be applied on the basis of fluence rate monitors positioned before and after the sample.<sup>(29)</sup> Moreover, given the high energy of the photons, this attenuation is mostly relevant for thick targets with high average atomic number.

Large sample photon activation analysis has many interesting aspects and advantages compared to LSNA, including its capability to detect elements such as C, N, and O, as well as Tl, Bi, and Pb. However, the number of photon activation analysis laboratories worldwide is very small and most of the large sample activation analysis studies are done with neutrons. For these reasons, this type of large sample analysis is not further elaborated upon in this article, and the reader is directed to the available literature.<sup>(29)</sup>

## 3 MEASUREMENT EQUATION OF LARGE SAMPLE NEUTRON ACTIVATION ANALYSIS

The basic measurement equations of NAA by which the mass of the unknown element is calculated directly demonstrates the fact that the technique does not set a priori constraints to the mass of the sample analyzed:

$$m_{\text{unk}} = m_{\text{std}} \frac{(A_{0,x})}{(A_s)} R_\theta R_\phi R_{\text{En}} R_\sigma R_{\text{nss}} R_\varepsilon R_{\gamma\text{ss}} R_{\text{inh}} \quad (1)$$

$$A_0 = \Phi_{\text{th}} \sigma_{\text{eff}} \frac{N_{\text{Av}} \theta m}{M} (1 - e^{-\lambda t_{\text{ir}}}) e^{-\lambda t_{\text{d}}} \frac{(1 - e^{-\lambda t_{\text{m}}})}{\lambda} \gamma \varepsilon \quad (2)$$

in which the subscripts “unk” and “std” refer to unknown and standard, respectively, and

$A_0$  = the area of the relevant peak in the  $\gamma$ -ray spectrum, corrected for differences in decay and measurement time between the unknown ( $x$ ) and the standard ( $s$ );

$R_\theta$  = ratio of isotopic abundance of the element of interest in test portion and standard (often = 1);

$R_\phi$  = ratio of thermal neutron fluence rates in test portion and standard;

$R_{\text{En}}$  = ratio of neutron energy distribution in test portion and standard;

$R_\sigma$  = ratio of effective activation cross sections for the test portion and standard at the different neutron energy spectra;

$R_{\text{nss}}$  = ratio of the neutron self-shielding in test portion and standard;

$R_\varepsilon$  = ratio of the photopeak efficiency for the test portion and standard;

$R_{\gamma\text{ss}}$  = ratio of the  $\gamma$ -ray self-attenuation in test portion and standard; and

$R_{\text{inh}}$  = ratio of the effect of extreme inhomogeneities in test portion and standard.

Also,

$\Phi_{\text{th}}$  is the thermal neutron fluence rate ( $\text{cm}^{-2} \text{s}^{-1}$ ),

$\sigma_{\text{eff}}$  is the effective absorption cross section ( $\text{cm}^2$ ),

$N_{\text{Av}}$  is the Avogadro's number ( $\text{mol}^{-1}$ ),

$\theta$  is the isotopic abundance,

$m$  is the mass of the irradiated element (g),

$M$  is the atomic mass number ( $\text{g mol}^{-1}$ ),

$\lambda$  is the decay constant of the radioisotope formed ( $\text{s}^{-1}$ ),

$t_{\text{ir}}$  is the irradiation duration (s),

$t_{\text{d}}$  is the decay time (s),

$t_{\text{m}}$  is the (live time) measuring time (s),

$\gamma$  is the abundance in the nuclear decay of the  $\gamma$ -ray measured, and

$\varepsilon$  is the full energy photopeak efficiency of the detector for the energy of the  $\gamma$ -ray measured.

Many of the correction terms,  $R_i$ , can often be neglected in normal sample analysis but some of them like  $R_{\text{nss}}$ ,  $R_{\gamma\text{ss}}$ ,  $R_\epsilon$ ,  $R_{\text{En}}$ , and  $R_{\text{inh}}$  become significant in large sample analysis. As such, algorithms in large sample NAA differ from normal NAA by the calculation/estimation of

- the neutron self-shielding and/or neutron fluence rate profile inside the test portion,
- the  $\gamma$ -ray self-attenuation,
- the volumetric photopeak source efficiency of the detector, and
- the impact of extreme inhomogeneity effects.

There are many approaches for these calculations, varying from pure theoretical modeling,<sup>(9)</sup> Monte Carlo modeling,<sup>(20)</sup> and modeling using a priori available information about the test portion composition<sup>(7)</sup> to pragmatic empirical estimations of the correction factors.<sup>(17)</sup> Modeling may even be avoided when, e.g., for routine applications a representative well-characterized (large sample) standard – even a reference material – is available.<sup>(18)</sup> These standardization methods are further discussed below.

## 4 INSTRUMENTATION

### 4.1 Neutron Sources for Large Sample Activation Analysis

The type and strength of the neutron source and energy characteristics play an important role in any type of NAA including LSNA, as the radioactivity produced is directly proportional to the neutron flux ( $\phi$ ) and energy-dependent neutron absorption cross section ( $\sigma$ ). The neutron source should provide a sufficiently high neutron fluence rate so as to keep the product of neutron fluence rate and large test portion mass almost equal to that in small test portion NAA. This criterion indicates that for test portions with masses in the order of 2 kg a neutron fluence rate of approximately  $5 \times 10^{12} \times 0.2/2000 = 5 \times 10^8 \text{ cm}^{-2} \text{ s}^{-1}$  would result in an adequate induced radioactivity during the irradiation time, similar to that applied in conventional NAA in which a 200 mg test portion is processed. Fluence rates on the order of  $10^8 - 10^{10} \text{ cm}^{-2} \text{ s}^{-1}$  are found at an extended distance from the core of small and medium-sized reactors,<sup>(15)</sup> in beam tubes, and in thermal columns (TCs).<sup>(5,19,20)</sup> However, low fluence rates can also be realized – or even may be preferred – by lowering the reactor power because of fuel economy considerations.<sup>(30)</sup> Table 2 also provides an indication of typical neutron sources available to provide the required neutron fluence rate.

The advantage of reactor TCs above, e.g., poolside facilities, is that the longitudinal neutron flux gradient

**Table 2** Typical neutron fluence rates for activation analysis of test portions of different mass along with neutron sources

Sample mass (g)	$n$ -flux ( $\text{cm}^{-2} \text{ s}^{-1}$ )	Neutron source
1–10	$2.10^{12} - 2.10^{11}$	Reactor
10–100	$2.10^{11} - 2.10^{10}$	Reactor
100–1000	$2.10^{10} - 2.10^9$	Reactor
>1 kg	$< 2.10^9$	Reactor, Isotopic $n$ -source $n$ -generator

$$(\text{Mass} \times \text{flux}) = \text{constant} = 200 \text{ mg} \times 10^{13} \text{ cm}^{-2} \text{ s}^{-1}$$

(i.e. horizontally away from the reactor core) over the sample is much less steep because of the multiple neutron scattering in the graphite inside the TC, as can also be derived from the differences in thermal neutron diffusion length in carbon and water, viz., 64.2 and 2.76 cm, respectively. Rotating the sample along its vertical axis compensates partly for these gradients. However, in some materials the neutron self-attenuation combined with the neutron flux gradient may result in situations in which the center of the test portion is hardly activated compared to the periphery. In such cases, the measured  $\gamma$ -rays originate mainly from the periphery and the analysis result will apply merely to the outermost layers of the sample rather than reflecting the bulk composition. In such facilities, the approach is to set limits to the dimensions of the test portion. Moreover, neutron self-moderation will occur owing to the less thermalized neutron spectrum in poolside facilities, resulting in difficulties in the calculation of the element amounts.

Neutron fluence rates  $< 10^{10} \text{ cm}^{-2} \text{ s}^{-1}$  may also be attainable with isotopic neutron sources and high-intensity neutron generators, and in (reactor-based) external neutron beams.  $^{252}\text{Cf}$  is probably the most attractive isotopic neutron source from the point of view of the neutron spectrum shape and easy thermalization aspects. However, the short half-life (2.64 years) may be seen as an economical disadvantage. Other isotopic neutron sources have a relatively hard neutron spectrum, resulting in relatively low thermal neutron fluence rate equivalents. The applicability of such neutron sources may, therefore, be limited to the determination of the major components in a sample.

Neutron generators (3–14 MeV) have their own scope of applications.<sup>(31,32)</sup> One of the problems in using neutron generators and isotopic neutron sources is that the neutron fluence is anisotropic and therefore the neutron flux seen by a large sample is not the same in all parts of the sample. This can be overcome to some extent by rotating the test portion during irradiation. Given the fact that the thermal neutron fluence rate in, e.g., a D-D

(deuterium ions on a deuterium target) generator is of the order of  $10^4$  lower than in research reactors, an increase in sample mass of at least  $10^4$  (i.e. from 200 mg to 2 kg) would be needed to compensate for this low thermal fluence rate.

An advantage of large (kilogram size) sample NAA with D-D generators over reactors is that the sample may be quickly removed from its irradiation position upon shutting down the accelerator, facilitating the measurement of radionuclides with short half-lives. For samples in the order of tens of grams, pneumatic facilities may be designed. Larger sample masses may also be considered for delayed neutron counting procedures to reach lower minimum detectable amounts, although this implies that a larger delayed neutron counter is needed too.

However, several technological obstacles exist both with isotopic neutron sources as with neutron generators, such as the large void needed within the moderator of the device. Moreover, since these moderators are often based on hydrogenous materials such as polyethylene or paraffin, steep flux gradients may occur over the sample, similar to those outlined earlier for poolside reactor facilities. The large sample approach may also be considered for irradiation with the sub-fast neutrons, although here an increase in sample mass from, e.g., 200 mg to 200 g might be sufficient for reaching the sensitivity required. However, an additional problem is that large sample masses will increase the effect of neutron self-moderation.

Most of the external neutron beams from nuclear reactor, with neutron fluence rates of  $10^6$ – $10^8$   $\text{cm}^{-2} \text{s}^{-1}$ , are suitable for PGNAA. An advantage associated with PGNAA is the flexibility in choosing the mass and shape of the test portion. However, one should be careful in increasing the test portion mass, as it might adversely affect the measurements because the background is sample dependent in PGNAA.<sup>(33)</sup> It becomes severe particularly in the cases where the hydrogen or boron fraction in the large test portion is high, as it results in an extremely intense source of prompt  $\gamma$ -radiation, which will affect the results.<sup>(34)</sup> External neutron beams of isotopic neutron sources have usually neutron fluence rates of  $<10^7$   $\text{cm}^{-2} \text{s}^{-1}$  and can in principle be used for PGNAA, though the energy definition becomes a tedious problem. Steep neutron gradients over the sample occur in neutron beam activation analysis too.

## 4.2 Irradiation Facility

Transferring the test portions to the irradiation position of the neutron source is usually done with pneumatic/hydraulic transfer facilities and/or manually or

automatic loading facilities. Most of the pneumatic facilities are designed to handle volumes up to 5–50 mL, which are placed in a sample carrier known as “rabbit”. Use of rabbit systems places constraints on the sample shape so as to maintain the defined geometry. In principle, it is possible to transfer test portions up to 1 kg or more through such facilities – such big systems already exist for transferring documents in offices and banks; however, it is yet to be explored and examined whether large rabbits can be obtained with the required specifications (quality of the rabbit materials, purity, and radiation/mechanical resistance) for application in reactors.

In some reactors TCs are available for accommodating a large sample irradiation facility (see Figures 1 and 2). Samples are placed in the irradiation position of the TC by the mechanical movement of a tray that houses the sample in a defined position.<sup>(5,19,20)</sup> In Table 3, suggestions for facilities for irradiation of test portions of different masses are indicated.

There are various design aspects to be taken into account for irradiation facilities:

1. A large-volume facility near the core of a nuclear reactor creates a void in the reactor's reflector, whereas loading and unloading may cause unwanted fluctuations in the core's reactivity. Moreover, a high amount of  $^{41}\text{Ar}$  will be produced from activation of the air in the container.
2. The thermal neutron fluence rate gradient in the water reflector of a light-water-moderated reactor is quite steep, typically by a factor of 3 per each 3 cm, which is due to the neutron diffusion length (2.84 cm) in water. Such a strong gradient would also create an unwanted strong flux variation over the large test portion to be activated. This may be corrected for by rotating the sample during counting,<sup>(5)</sup> by mixing the sample after irradiation,<sup>(17)</sup> or by the use of *in situ* relative efficiency method.<sup>(19)</sup> Mixing, however, eliminates information about inhomogeneities. The problem of heterogeneity may also be addressed by dividing the large test portion into many smaller fractions, to be processed individually followed later on by combining of the results.
3. Large hydrogen mass fractions may result in neutron spectrum changes over the test portion volume due to self-thermalization. This phenomenon is difficult to correct for mathematically, and may be an additional reason to consider an irradiation facility with well-thermalized neutron spectrum, for instance, to be realized in a TC.
4. Large sample activation facilities at isotopic neutron sources must be designed in such a way that adequate shielding is ensured against the prompt  $\gamma$ -rays, which will be several orders of magnitude higher than with normal small samples.

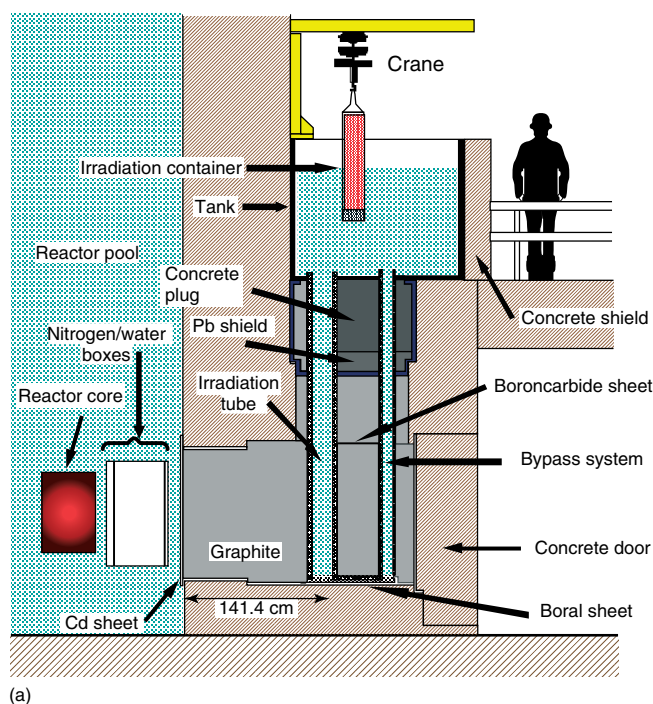


**Figure 1** Schematic drawing (a) and picture of model (b) of the large sample neutron activation analysis facility in the thermal column of the Hoger Onderwijs Reactor in Delft.

A few of the large sample NAA reactor facilities that are currently operational are given in Table 4.<sup>(35)</sup> Large sample PGNA facilities have been realized in Hungary and Japan. Isotope neutron source-based large sample PGNA facilities are in use in some places.<sup>(36)</sup>

#### 4.3 Sample Containers for Irradiation

The large sample container itself may be of any shape and type. A wide-neck bottle is easy to fill when coarse

material has to be analyzed (Figure 3).<sup>(5)</sup> A container of inexpensive plastic may be preferred, as the impurities in the plastic itself (blank contribution) may be neglected at a given sample size (see Table 5). If the contribution from the sample holder is substantial, the irradiated large samples may also be easily transferred after irradiation into nonirradiated containers and possible small losses during transfer can be neglected in view of the large mass of the test portion. As such, a Marinelli beaker geometry or multisample container (Figure 4)<sup>(37)</sup> may

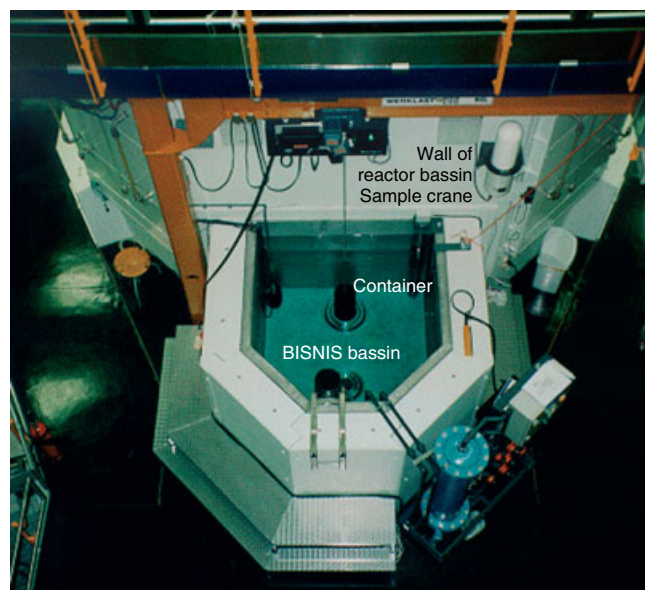


**Figure 2** Top view of the large sample activation analysis facility in Delft.

have certain advantages, depending on the application (see below).

#### 4.4 Counting Facility

Very large Ge detectors are available (crystal sizes up to 400–800 cm<sup>3</sup>, comparable to “relative efficiencies” of 100–200%). Such big detectors are an additional tool to maintain adequate sensitivity in NAA. Side-looking detectors (“horizontal dipstick”) have the advantage

**Table 3** Irradiation facilities needed for test portions of different masses

Test portion mass (g)	Type of facility
1–10	Existing pneumatic facility
10–100	Existing/special pneumatic facility
100–1000	Existing manual loaded or special facility such as the thermal column of a reactor
>1000	Often a new special facility

that cylindrical samples, positioned perpendicular to the detector axis, can easily be rotated around the sample axis to reduce geometrical effects. Vertical dipstick detectors have the advantage to measure large samples in the Marinelli beaker geometry. Well-type Ge detectors can handle test portion volumes of up to approximately 8 mL, and thus have their own niche in large sample NAA, especially as an addition to enhance sensitivity for test portions in the grams range.

In general, it is preferable to count the large sample by placing it at a certain distance from the detector end cap to minimize complications in the efficiency calculations, in particular in the coincidence summing corrections. The distance between the test portion and detector is guided by the sample activity; the higher the activity, the farther the sample to be placed from the detector. Automatic sample changing can be realized irrespective of the sample size. Sample changers are already commercially available for containers with volumes up to 1 L, although they have been designed for the Marinelli beaker measurement.

**Table 4** Details of some of the irradiation facilities used for LSNA<sup>(37)</sup>

Institute	Nation	Reactor type	Test portion mass	Facility (TC = thermal column)	Neutron fluence rate (cm <sup>-2</sup> s <sup>-1</sup> )
Dalhousie University	Canada	SLOWPOKE	30 g	Rabbit system	2.5 × 10 <sup>11</sup>
International Centre for Environmental and Nuclear Sciences	Jamaica	SLOWPOKE	30 g	Rabbit system	2.5 × 10 <sup>11</sup>
University of the West Indies					
Atominstytut	Wien, Austria	TRIGA	5 g	Fast and normal Rabbit system	2 × 10 <sup>12</sup>
FRG-II	Munich, Germany	TRIGA	1 kg	Manual loading	6 × 10 <sup>9</sup>
Delft University of Technology, Reactor Institute Delft	Netherlands	Swimming pool reactor	50 kg	Manual loading, TC	3 × 10 <sup>8</sup>
BARC, Mumbai	India	Swimming pool reactor, Apsara	1–4 kg	Manual loading, TC	2 × 10 <sup>8</sup>
Demokritos	Greece	Swimming pool reactor	2 kg	Manual loading, TC	5 × 10 <sup>6</sup>
Institute of Nuclear Physics	Kazakhstan	Pool type reactor	10 × 100 mL	Manual loading, core	Low power operation



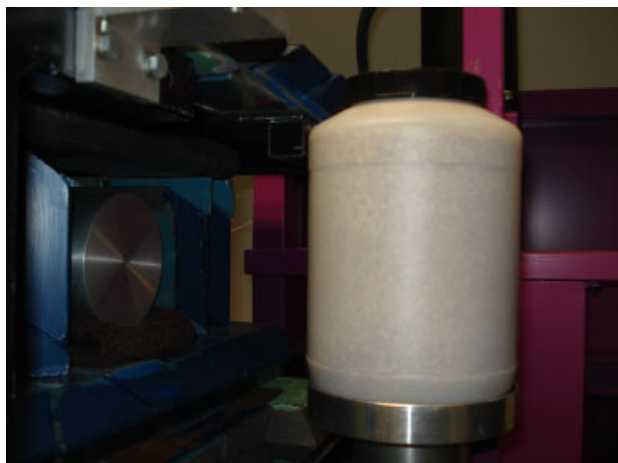


**Figure 3** Large sample container (diameter 12 cm, height 20 cm) in front of side-looking Ge detector (cryostat diameter 9 cm).

**Table 5** Typical masses of test portions and required bottles, indicating the reduction of the ratio of masses in the case of large sample NAA

Bottle volume (mL)	Bottle mass	Sample mass	Sample mass/bottle mass
0.5	0.2 g	0.2–0.4 g	1–2
50	10	30–60	3–6
100	15	60–120	4–8
250	25	150–300	6–12
500	37	300–500	8–15
1000	100	600–1000	6–10

Adequate shielding of the stored samples remains, of course, a prerequisite.

Different detector calibration approaches are needed – taking into account voluminous photo peak efficiency,  $\gamma$ -ray self-attenuation, and coincidence summing correction if Marinelli beaker geometries or multisample containers are applied. In the multisample container setup, as the geometry for each container is the same, one can start with one container and measure up to 20 samples according to their decay.

The spectrometer may have to be equipped with a separate device to allow the determination of the effective  $\gamma$ -ray linear attenuation coefficients using a multi- $\gamma$ -ray pencil beam of an external source (e.g.  $^{152}\text{Eu}$ ). An example of such a setup is given in Figure 5.

It may be necessary to collimate the detector in case the localization of the inhomogeneity is the subject of interest in large sample analysis (see Figure 6). Such a setup will allow, in principle, for emission tomography of the activated sample.<sup>(38)</sup>

More advanced spectrometer systems may be designed, in which two or more Ge detectors surround the large sample to create nearly  $4\pi$  geometry of the detectors.<sup>(29)</sup>

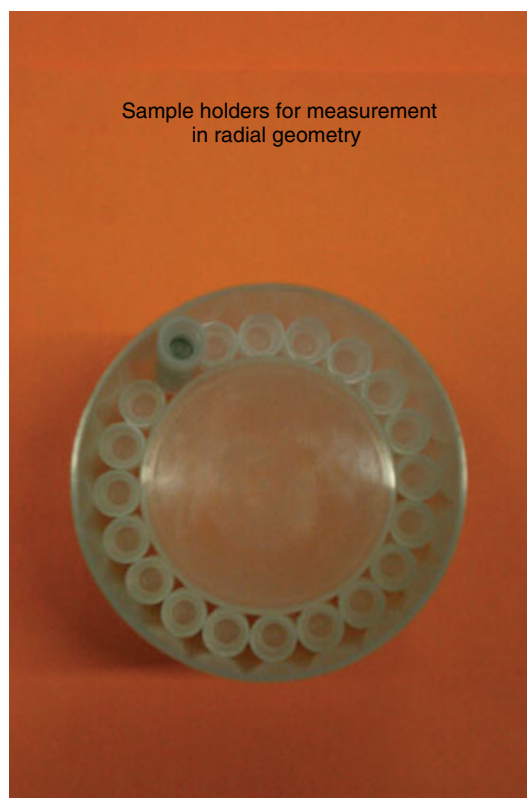


**Figure 4** A multisample container.<sup>(37)</sup>

The individual spectra can be added later to create a composite spectrum with better statistics.

The  $\gamma$ -ray spectrometer should be equipped with dedicated high-count-rate electronics if the induced radioactivity to be measured would result in a count rate  $>20\,000\text{ s}^{-1}$ . The prerequisites are a transit–reset preamplifier and pulse processing electronics (analog or digital), allowing for on-line dead-time compensation, e.g., based on the loss-free counting principle.<sup>(39)</sup> The latter is relevant only if count rates vary significantly during the counting time, as may be the case in counting radionuclides with very short half-lives (in the range of seconds to several minutes).

It is interesting to take note that there are a few applications where counting could be carried out using well-type scintillation detectors. In the cases where major components only have to be analyzed and the neutron sources are isotope based, then the resulting activity could be low and the  $\gamma$ -ray spectra might be relatively simple, which could be measured using high-efficiency scintillation detectors. Large sample NAA with isotopic sources and the use of scintillation detectors may be considered as an additional opportunity to further enhance the sensitivity. One may even construct a simple  $4\pi$  detector by putting two well-type detectors against each other.

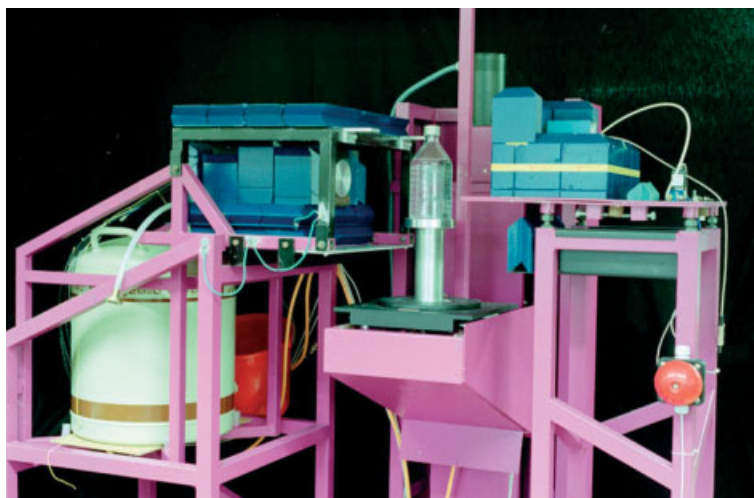


**Figure 5** Large sample  $\gamma$ -ray spectrometer with (from left to right) the shielded side-looking Ge detector, the sample on the rotating turntable, and the lead shield with the  $^{152}\text{Eu}$  source for  $\gamma$ -ray transmission. The source can be pneumatically moved in front of a point-source collimator.<sup>(1)</sup>

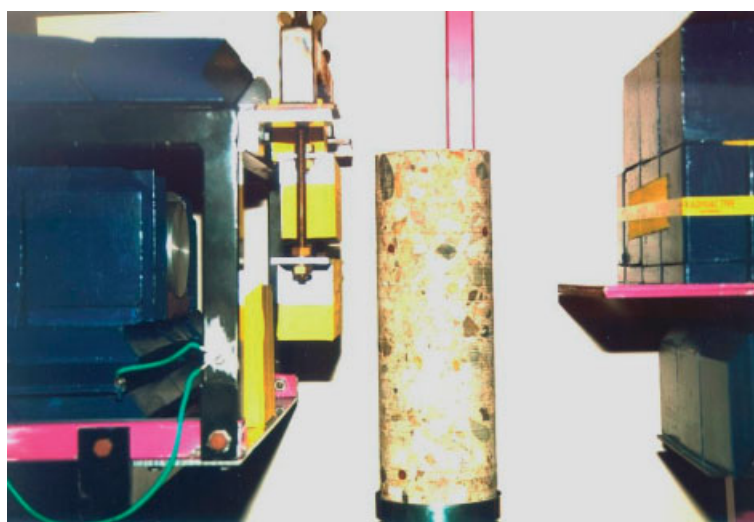


**Figure 6** Close-up view of the  $\gamma$ -ray spectrometer showing (from left to right) the shielded Ge detector, a slit collimator, a (simulated) large sample, and the lead shield for the transmission source.<sup>(1)</sup>

## 5 CALIBRATION

Determination of the elemental masses in large sample NAA may be done as in small sample NAA, via

- the absolute method,
- the comparator method, or
- the internal standard method.

### 5.1 Absolute Method

The absolute method for standardization in NAA is based on using known values for neutron fluence rate and activation cross sections, derived either from previously performed measurements or from reactor

physics estimations (neutron fluence rate) and from the literature data (cross sections); the same is the case with  $\theta$ ,  $N_{Av}$ ,  $M$ ,  $\sigma_{\text{eff}}$ ,  $\gamma$ , and  $\lambda$ . For many (n, $\gamma$ ) reactions and radionuclides, the parameters  $\sigma_{\text{eff}}$ ,  $\gamma$ , and  $\lambda$  are not precisely known, while in some cases  $\theta$  also is not known accurately. Since the various parameters are often achieved via independent methods, their individual imprecisions will add up in the calculation of the elemental amounts, leading to large systematic errors. This method is best applicable if the composition of the sample matrix is well established in advanced, as is the case, e.g., when dealing with pure materials. It is well known that even in normal NAA this approach may not yield highly accurate data but still the results may be adequate

for the intended purpose. Still, additional estimates are needed for correcting the neutron fluence rate gradient and the  $\gamma$ -ray self-absorption. The first may be done using simplified models or using neutron transport codes, and the second after simple transmission measurements or using tabulated linear attenuation coefficients in case the sample is well defined with respect to its composition.

## 5.2 The Comparator Method

The test portion is irradiated together with a calibration sample containing a known amount of the element(s) of interest. The calibration sample is measured under (preferably) the same conditions as the sample (sample-to-detector distance, sample size, and if possible composition). From a comparison of the net peak areas in the two measured spectra, the mass(es) of the element(s) of interest can be calculated (see above, Equations (1) and (2)):

$$mass_{\text{unk}} = mass_{\text{std}} \frac{(A_{0,x})}{(A_s)} R_\theta R_\phi R_{\text{En}} R_\sigma R_{\text{nss}} R_\varepsilon R_{\gamma\text{ss}} R_{\text{inh}} \quad (3)$$

The relative standardization based on element standards is not immediately suitable for laboratories aiming at the full multielement powers of INAA. It is virtually impossible to produce a multielement standard containing known amounts of all 70 detectable elements with sufficient accuracy in a volume closely matching the size and the shape of the samples. For this reason, some laboratories prefer to use (certified) reference materials as a multielement standard. However, if dealing with large samples (gram to kilogram size), the use of (certified) reference materials is not practical (major differences may exist in neutron spectrum characteristics in the real sample and in the standard), economical (reference materials are expensive and large sample analysis would imply a high consumption rate), or ethical (certified reference materials are produced for method validation purposes, not necessarily for calibration).

Multielement INAA based on the relative standardization method is feasible when performed according to the principles of the single comparator method. Assuming that all relevant experimental conditions are stable over time, standards for all elements are co-irradiated, each in turn with the chosen single comparator element. Once the sensitivity for all elements relative to the comparator element has been determined (expressed as the so-called  $k$ -factor, see Section 5.3), only the comparator element has to be used in routine measurements instead of individual standards for each element.

## 5.3 Single Comparator Method

Originally, the single comparator method for multielement INAA was based on the ratio of proportionality factors of the element of interest and of the comparator element after correcting for saturation, decay, counting, and sample weights. Girardi et al.<sup>(40)</sup> defined the  $k$ -factor as

$$k = \frac{M_t \gamma_c \varepsilon_c \theta_c \sigma_{\text{eff},c}}{M_c \gamma_t \varepsilon_t \theta_t \sigma_{\text{eff},t}} \quad (4)$$

in which the subscripts “t” and “c” refer to the element of interest in the sample and comparator, respectively. Mass fractions can then be calculated from these  $k$ -factors; for an element determined via a directly produced radionuclide, the mass fraction  $\rho$  follows from

$$\rho = \frac{(A/\text{SDCw})_t}{(A/\text{SDCw})_c} \cdot k \quad (5)$$

where  $S = (1 - e^{-\lambda \cdot t_{\text{ir}}})$

These experimentally determined  $k$ -factors are often more accurate than those calculated on basis of literature data as in the absolute standardization method. However, the  $k$ -factors are valid only for a specific detector, a specific counting geometry, and the irradiation facility and remain valid only as long as the neutron flux parameters of the irradiation facility remain stable.

The main problem of the single comparator method in LSNAA is that differences in neutron exposure,  $\gamma$ -ray attenuation, and volumetric counting efficiency between comparators and samples all have to be accounted for. In normal NAA, most of these differences can be neglected, also because the comparators are co-irradiated with the samples. But in LSNAA this may be practically impossible; the irradiation facility may not be spacious enough, and substantial difference may exist in the neutron exposure and flux gradients. Only if the neutron flux spectrum is well known – as in TCs – and the neutron fluence rate gradient can be established in each individual test portion, the comparator method provides an opportunity for applicability. In that case, even the  $k_0$ -based method for standardization may be applied.

The comparator method is, however, very well usable for large sample analysis of, e.g., large liquid samples such as water or oil since standard samples with element spikes into a similar matrix can easily be prepared.

## 5.4 $k_0$ -Based Method for Standardization

At the Institute for Nuclear Sciences in Ghent, Belgium, an attempt has been made to define  $k$ -factors that should be independent of neutron flux parameters as well as spectrometer characteristics.

The expression for the activation reaction rate can be written as

$$R = \Phi_{\text{th}}\sigma_0 + \Phi_{\text{epi}}I_0(\alpha) \quad (6)$$

The ratio  $f$  of the thermal neutron flux and the epithermal neutron flux is  $f = \Phi_{\text{th}}/\Phi_{\text{epi}}$  and the ratio of the resonance integral and the thermal activation cross section can be expressed as  $Q_0(\alpha) = I_0(\alpha)/\sigma_0$ ; thus the effective cross section is

$$\sigma_{\text{eff}} = \sigma_0 \left( 1 + \frac{Q_0(\alpha)}{f} \right) \quad (7)$$

The  $k_0$ -factor is now defined as

$$k_0 = \frac{1}{k} \frac{1 + (Q_{0,c}(\alpha)/f) \varepsilon_c}{1 + (Q_{0,t}(\alpha)/f) \varepsilon_t} = \frac{M_c \theta_t \sigma_{0,t} \gamma_t}{M_t \theta_c \sigma_{0,c} \gamma_c} \quad (8)$$

and the mass fraction, again for an element determined via a directly produced radionuclide, is found from

$$\rho = \frac{1 + (Q_{0,c}(\alpha)/f) \varepsilon_c}{1 + (Q_{0,t}(\alpha)/f) \varepsilon_t} \frac{(A/\text{SDCW})_t}{(A/\text{SDCW})_c} \frac{1}{k_0} \quad (9)$$

The  $k_0$ -factor has thus become a purely nuclear parameter for the thermal neutron spectrum. In the  $k_0$  convention, Au is proposed as the comparator element. The neutron flux parameters  $f$  and  $\alpha$  no longer cancel out in concentration calculations and must be measured in each irradiation facility, preferably even for each irradiation and sample.<sup>(41)</sup> The  $k_0$ -factors are used in Delft for the analysis of very large samples.

### 5.5 Internal Monostandard Method

In the internal monostandard method, one of the radionuclides produced during activation of the test portion is used as monostandard. The rationale behind this is that the effect of neutron spectrum perturbation is the same for this parent element of this radionuclide as well as for all other elements in the sample; as such there is an implicit assumption that the test portion is “macroscopically” homogeneous.

In the case of internal monostandard method using TC irradiations followed by  $\gamma$ -spectrometric method, the ratio of mass ( $m$ ) of an element ( $x$ ) in the test portion ( $t$ ) to mass of the internal comparator element ( $c$ ) in the sample is given by Equation (10):

$$\frac{m_t}{m_c} = \frac{((\text{S.D.C}) \cdot (f + Q_o(\alpha)))_c}{((\text{S.D.C}) \cdot (f + Q_o(\alpha)))_t} \cdot \frac{A_{At}}{A_{Ac}} \cdot \frac{(\varepsilon_\gamma)_t}{(\varepsilon_\gamma)_c} \cdot \frac{1}{k_{0,c}(x)} \quad (10)$$

Here,  $k_{0,c}(x)$  represents the relative sensitivity of element  $x$  with respect to  $y$  and is calculated from the  $k_{0,Au}$  factors in the literature.

The internal monostandard method either results in elemental mass ratios (element of interest vs. monostandard element) and thus may serve for comparative studies, or, in the case of, e.g., materials of high purity and known stoichiometry, directly into mass fractions of the elements of interest if (one of) the major component(s) is used as the monostandard element.

### 5.6 Neutron Fluence Rate Monitoring

Neutron fluence rate monitoring is needed for the  $k_0$  method of standardization and may be done noninvasively with the flux monitors outside the sample, as well as by inserting flux monitors inside the sample. The first approach may use, e.g., the neutron depression outside the large sample to estimate the neutron flux distribution;<sup>(42)</sup> the second approach provides direct information on the flux distribution.<sup>(43,44)</sup> The first approach is applied in Delft for large sample irradiations in the reactor's TC.<sup>(5)</sup> During the irradiation, the sample is surrounded by four flux monitors at any desired height around the sample. Since the unperturbed neutron flux gradient in the TC can be derived from the irradiation of a pure graphite sample, the neutron flux depression outside the sample can be estimated (Figure 7). This forms the basis for estimating the effective neutron diffusion length and neutron diffusion coefficient. Finally, the overall correction factor is calculated – which reflects how the large sample compares to a small sample – using the volume efficiency of the Ge

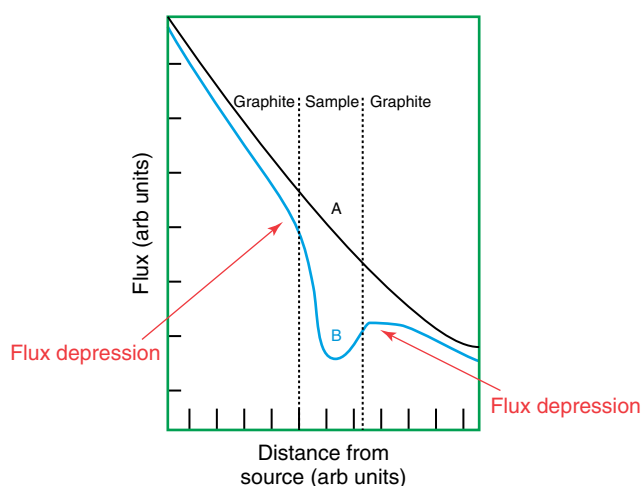


**Figure 7** Neutron flux depression outside a large sample placed inside the graphite-filled thermal column. The curve A indicates the unperturbed flux gradient; curve B schematically shows the flux gradient if a sample absorbing and scattering thermal neutrons is placed in the irradiation position.

detector, the neutron diffusion length and coefficient, and the effective linear attenuation coefficients.

Changes in the neutron spectrum due to self-thermalization are much more difficult to deal with, as these are not easy to monitor. The extent of this effect depends, of course, on the neutron spectrum shape and the fraction of epithermal and fast neutrons compared to the thermal neutrons. In TC facilities, the ratio of thermal over nonthermal neutrons may be much larger than a factor of 1000, eliminating the significance of neutron self-thermalization. The user of the irradiation facility should be familiar with this phenomenon, and a priori information must always be collected about the sample composition so as to estimate the extent of these effects and to decide if empirical correction factors can be applied or if additional in situ monitoring is needed (i.e. invasive, by inserting suitable monitors inside the sample).

### 5.7 $\gamma$ -Ray Self-Attenuation

The  $\gamma$ -ray self attenuation correction is relatively easy to establish once the effective linear attenuation coefficients are available, either by measurement or by calculation from the approximate (or well-known) elemental composition. A multi- $\gamma$ -ray emitting source, with  $\gamma$ -ray energies distributed over the entire range of interest (such as  $^{152}\text{Eu}$ ,  $^{182}\text{Ta}$ ) can be used for this. A nearly pencil beam geometry can be created by locating this source behind a pinhole collimator, and the  $\gamma$ -ray transmission can be measured at several heights along the sample. This forms the basis for the estimation of the effective linear  $\gamma$ -ray attenuation coefficients.

The volumetric photopeak efficiency can be determined by Monte Carlo modeling, but this requires precise information about the inner geometry of the cryostat and detector configuration (including the dead-layer thickness). Empirical curves may be determined using standard sources in water, as the self-attenuation can simply be subtracted from the measured efficiency. In situ relative detection efficiency in a voluminous sample was determined using the multi- $\gamma$ -emitters produced in the sample, and was adequate to calculate mass ratios with respect to the comparator using Equation (5).<sup>(45)</sup>

Pragmatic approaches have been suggested in which the large sample, after activation, is repacked into many small-diameter containers that are placed in a cylindrical holder surrounding the detector. If the detector crystal is perfectly symmetrically mounted inside the cryostat, the detection efficiency for each of the positions around the detector is the same, which simplifies the calculations. Besides, the dimensions of the small containers can be chosen such that  $\gamma$ -ray attenuation effects may be neglected.

It should be noted that the  $\gamma$ -ray spectrum due to the natural radioactivity of the sample material has also to be measured in large sample analysis, prior to the activation. These "sample background" peaks in the  $\gamma$ -ray spectrum should be separately treated later on in the neutron and  $\gamma$ -ray self-attenuation corrections.

### 5.8 Extreme Inhomogeneities

Combination of correction algorithms for neutron and  $\gamma$ -ray self-attenuation as well as for the volumetric photopeak efficiency yields an "overall correction factor", which reflects the difference between the actual detector response for a given  $\gamma$ -ray energy and the theoretical detector response if the sample were a massless point source located in the large sample's center, without any neutron and  $\gamma$ -ray attenuation.<sup>(9)</sup>

In these corrections, it is assumed implicitly that both trace elements and major (matrix) elements in the sample are homogeneously distributed on a macroscopic scale. If this condition is not met, there is a high probability that owing to the neglect of inhomogeneities the concentrations determined are not correct. How large these deviations may be as a result of such neglect has been studied via computer simulations. Inhomogeneities may influence the results of the irradiation as well as of the measurement; therefore, both have been treated separately. Inhomogeneous matrix composition has been modeled by composing a sample of cylinders with strongly differing neutron or  $\gamma$ -ray attenuation properties. Inhomogeneity for trace elements has been simulated by modeling extreme distributions of a trace element with either neutron or  $\gamma$ -ray attenuation properties, strongly differing from those of the main composition of the sample.<sup>(20,46)</sup> Both inhomogeneities in matrix composition (e.g., layered structures) and trace-element inhomogeneities (e.g., "hot spots") were taken into account.

Obviously, the results of these simulations demonstrated that false concentrations may be obtained if inhomogeneities are not accounted for in the interpretation step of large sample INAA. The smallest errors may occur for matrix inhomogeneities; the most pronounced effects can be expected when the trace element of interest is distributed either on the outside or on the axis of the cylindrical sample.

In these simulations, materials or elements were selected with neutron and  $\gamma$ -ray attenuation properties that were strongly different from the rest of the sample; as such they may be considered as "extremities", and the consequences on the inaccuracy of the results rather indicate "worst case" conditions.

### 5.8.1 Determination of Inhomogeneities

The presence of extreme inhomogeneities in large samples may be considered a nuisance. On the other hand, large sample analysis is a unique tool for determining these inhomogeneities without destroying the test portion. To this end, sample scanning using a collimated detector has been introduced, and it is assumed that the sample consists of volume elements that individually are considered homogeneous.

The set of spectra constituting one scan is statistically evaluated to determine whether fluctuations over the scan of the count rates of  $\gamma$ -rays of a given energy are only due to Poisson counting statistics or are also due to inhomogeneities in the sample. If inhomogeneities have only a layered structure in the direction of the cylinder axis of the sample, the sample can be analyzed layer by layer, and for the most extreme cases the analysis can be performed for each voxel separately. An example of a collimated detector system for large sample scanning is shown in Figure 6.

Baas et al.<sup>(38,47)</sup> developed a method for the detection of local inhomogeneities. The count rate in each channel of each segmented measurement can therefore be compared with the average count rate in each channel after summing all individual measurements. Such a comparison, taking into account uncertainties, is made analogous to the  $\zeta$ -score principle. Values of  $|\zeta| > 2$  or  $> 3$  (depending on the analyst's fitness-for-purpose criterion) indicate a local inhomogeneity at the respective  $\gamma$ -ray energy in a particular voxel. This approach is visualized in Figure 8. A bottle of approximately 25 cm length and 8 cm diameter filled with soil was irradiated in the large sample facility

in Delft. The induced radioactivity was measured with a 96% Ge detector, collimated with a 10-cm-thick Pb collimator with a 2-cm split opening. The figure shows the  $z'$  scores for each channel number ( $\gamma$ -ray energy) along the height of the sample. From the zoomed details it can clearly be seen that strongly deviating  $\zeta$ -scores occur at, e.g., 439 and 1115 keV, indicating an inhomogeneity for zinc. In addition, the histogram of all  $\zeta$ -scores in this figure provides also an insight into the presence of this inhomogeneity.<sup>(47)</sup>

## 6 QUALITY CONTROL

The high degree of accuracy in normal activation analysis results from decades of experience in the development of certified reference materials. Many sources of error and the quantification of their impact are known.<sup>(48,49)</sup> Methods commonly referred to as *quality control practices* have been developed to inspect the occurrence of errors during the analysis, whereas implementation of quality assurance contributes to minimizing and even avoiding the occurrence of errors. The known sources of error in normal activation analysis may occur in large sample analysis too. Some of them – such as  $\gamma$ -ray self-attenuation and neutron/photon fluence rate, or neutron spectrum gradients – have much larger effects. Extreme inhomogeneities are an additional phenomenon in large sample analysis,<sup>(46)</sup> with an impact on the degree of accuracy.

Quality control in normal activation analysis includes the simultaneous analysis of well-characterized quality

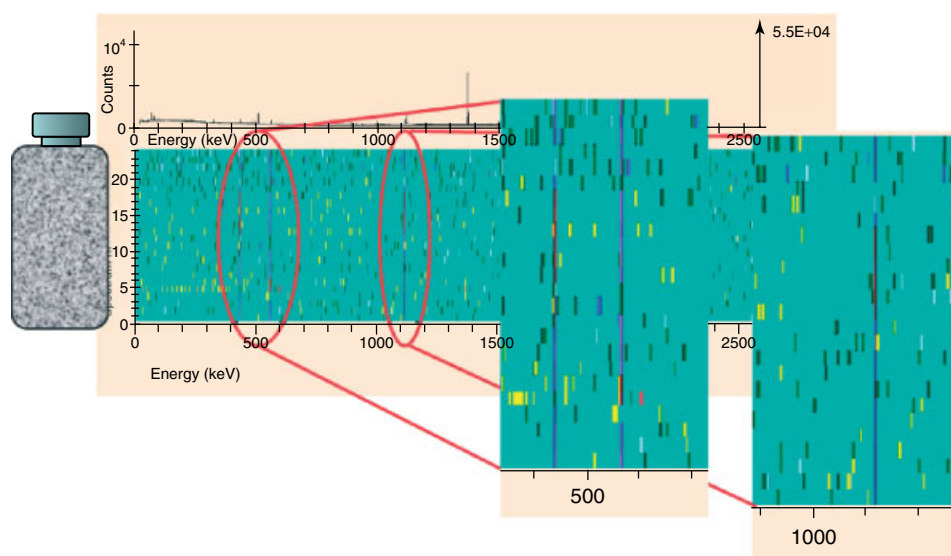


**Figure 8** Energy- and position-correlated  $\zeta$ -scores (see text) of measured radioactivity, indicating location of inhomogeneities in a sample of 20 cm height and 10 cm diameter.

**Table 6** Opportunities of quality control measures traditionally applied in normal activation analysis for samples of larger sizes

	Quality control samples	Blanks	Duplicates	$\gamma$ -Ray intensity ratios and multiple radio nuclides
1 g	Y	Y	Y	Y
10 g	N	Y/l.r.	Y/n.r.	Y
100 g	N	l.r.	n.r.	Y
1 kg	N	l.r.	n.r.	Y

Y = yes, application possible; N = no, not possible; l.r. = less relevant (see text); n.r. = not relevant.

control samples, blanks, and sometimes duplicates. In addition, inspection of the intensity ratios of  $\gamma$ -ray peaks of a given nuclide and/or the quantified results based on different radionuclides formed from a given element also provide a unique opportunity to inspect for errors. The applicability of these quality control approaches for samples of increasing mass is given in Table 6.

It is clear that basic problems emerge when extending the traditional approaches to samples with weights of more than a few grams. Firstly, well-characterized control samples of the size of large samples (several grams to kilograms) are either very expensive to use or not available at all. Secondly, large sample analysis may be required because of the heterogeneity of the object, which cannot be simulated by a control sample even if it were available. Thirdly, duplicates – assuming identical composition in mass fraction and in degree of homogeneity – may probably not be available when larger sample masses are needed. The problem related to the blank – impurities in the sample container and/or contamination – has, on the contrary, a smaller impact on the final result since the increase in the ratio of sample mass to container mass may result in negligible contribution of the blank (Table 5).

New strategies have to be developed to control the analytical quality in large sample analysis. One of the opportunities is to continue with the use of performance indicators, derived from the actual sample analyzed. In fact, this is not different from most quality control procedures in, e.g., manufacturing and production, in which the quality of a final product depends on predefined specifications being met, such as dimensions, tolerances, mass, color, or operation characteristics. The inspection of  $\gamma$ -ray intensity ratios and the use of different radionuclides of one element are already examples of such a form of quality control in activation analysis. This approach can further be extended to other sample/material characteristics on the basis of physical sample properties such as  $\gamma$ -ray self-attenuation and

neutron attenuation parameters, as well as via the degree of inhomogeneity (Table 3).

### 6.1 Quality Control in Large Sample Analysis

Some materials may be difficult to be processed to such homogeneity that representative subsamples can be taken at the <1 g level. For such materials, it may be advantageous to analyze much larger quantities without homogenization and to assume that the inhomogeneities are randomly distributed throughout the sample, so that the entire quantity can be considered as homogeneous. However, this assumption has some limitations. Overwater and Bode demonstrated the impact of extreme inhomogeneities on the correction mechanisms for the attenuation of  $\gamma$ -ray attenuation and neutron self-shielding.<sup>(46)</sup> Inhomogeneities with strong  $\gamma$ -ray absorbing properties have stronger effects on the degree of accuracy than those with strong neutron absorbing properties. It is therefore relevant to inspect for the presence of such extreme inhomogeneities in order to decide on the value of the finally calculated mass fractions. Two opportunities to inspect such inhomogeneities are given here.

The effective linear  $\gamma$ -ray attenuation coefficient is usually determined by measuring the transmission of  $\gamma$ -rays of different energies emitted by an external source with known emission rates.<sup>(9,45)</sup> The values of the effective linear attenuation coefficients may be estimated using the tabulated values for the elements. Typically, for example, biological and geological material values of  $\sim 0.15 \text{ cm}^{-1} < \mu < \sim 0.60 \text{ cm}^{-1}$  at  $\sim 100 \text{ keV}$ ;  $\sim 0.12 \text{ cm}^{-1} < \mu < \sim 0.25 \text{ cm}^{-1}$  at  $\sim 300 \text{ keV}$ ; and  $\sim 0.05 \text{ cm}^{-1} < \mu < \sim 0.15 \text{ cm}^{-1}$  at  $\sim 1000 \text{ keV}$  can be found. A “bandwidth” of the linear attenuation coefficient can thus be determined at different  $\gamma$ -ray energies for different types of materials (e.g. environmental, geological) (Figure 9). This can assist in inspecting whether the experimentally determined attenuation coefficients have realistic values. Moreover, if scanned measurements are carried out, an indication of local (layer-type) inhomogeneities with strong  $\gamma$ -ray absorbing properties may already be obtained. An example of this approach is given in Figure 10. The transmission of the  $\gamma$ -rays of a  $^{152}\text{Eu}$  source was measured at different heights along a  $\sim 1\text{-m}$  long,  $\sim 15\text{-cm}$  diameter soil drill core sample prior to neutron activation. The effective linear attenuation coefficients for each of the  $\gamma$ -ray energies were fitted with a polynomial so as to estimate the effective linear  $\gamma$ -ray attenuation at other  $\gamma$ -ray energies. The attenuation coefficients at 100, 300, and 1000 keV all fall within the expected bandwidths. There are no indications in this example for layer inhomogeneities with strongly differing  $\gamma$ -ray absorbing properties.

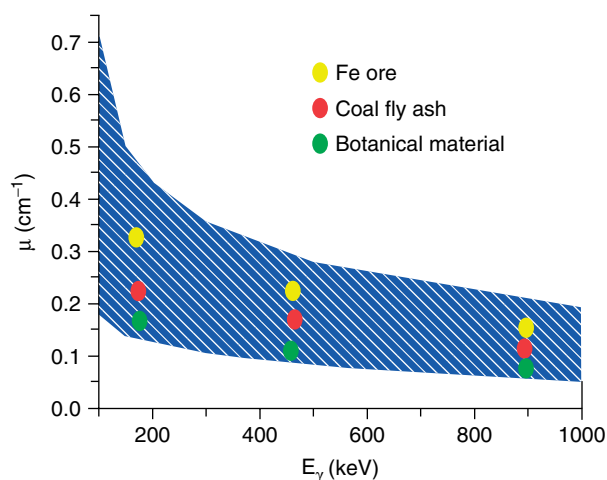


**Figure 9** Range of linear  $\gamma$ -ray attenuation coefficients for typical materials.<sup>(50)</sup>

Additionally, the methods developed by Baas et al. (described in the preceding text) can be used for the detection of local inhomogeneities. It can now be decided on a case-to-case basis whether such inhomogeneities have any unwanted impact on the final analysis result.

The correction for neutron self-shielding in LSNA may be made using information derived from the neutron fluence rate depression at positions in the irradiation facility just outside the sample. Overwater and Hoogenboom<sup>(42)</sup> developed this approach to estimate the thermal neutron diffusion length  $L_s$  and the thermal neutron diffusion coefficient  $D_s$ , which subsequently were used to reconstruct the neutron fluence rate profile inside the large sample. Both  $L_s$  and  $D_s$  are physical

element properties and, similar to the effective linear  $\gamma$ -ray attenuation coefficient, boundaries can be estimated for the values of these two parameters in real materials. Though strongly correlated ( $L_s^2 = D_s/\Sigma_a$ , with  $\Sigma_a$  the macroscopic absorption cross section ( $\text{cm}^{-1}$ )), typical values are  $\sim 1 \text{ cm} < L_s < \sim 20 \text{ cm}$  and  $\sim 0.2 \text{ cm} < D_s < \sim 3 \text{ cm}$ . An example is given in Figure 4. A  $\sim 1\text{-m}$  long,  $\sim 15\text{-cm}$  diameter water basin sediment drill core was analyzed in the frame of a pollution research project. Zinc foils were used as neutron flux monitors. The monitors were positioned just outside the sample container to monitor neutron fluence rate depression by comparison with the neutron fluence rates as monitored in a separate irradiation with a solid graphite sample, thus simulating the unperturbed neutron flux. The calculated values of  $L_s$  and  $D_s$  at different heights are plotted within the bandwidths for these values (Figure 11). Also, the average neutron fluence rates as a function of sample height is given. The fluence rates can be fitted with a cosine function, reflecting the flux distribution within the reactor's TC.

Assuring the quality of the results requires insight, monitoring, and control of the sources of error. Quality control procedures as traditionally applied in chemical analysis are not fully applicable in large sample analysis.<sup>(50)</sup> One of the advantages of activation analysis is that some of the measured sample parameters dealing with  $\gamma$ -ray and neutron attenuation can only vary in ranges set by well-known values of elemental constants. These parameters can be much more easily determined in large sample analysis than with samples in the milligram range, thereby offering an outlook for direct verification of the quality of the related correction algorithms.

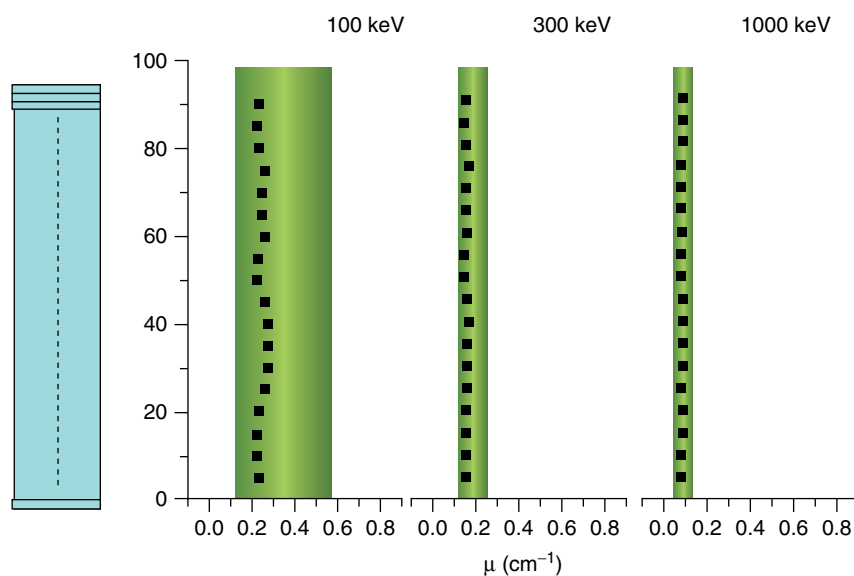


**Figure 10** Measured linear attenuation coefficients at 100, 300 and 1000 keV of a 15 cm thick soil drill core.



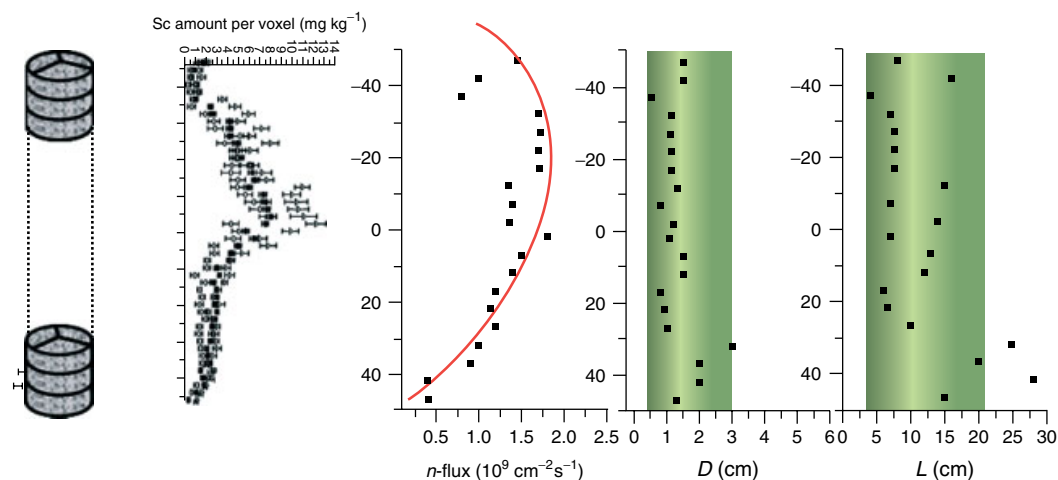


**Figure 11** Results of collimated large sample analysis of a stack of soil samples, total of 1 m length, 12 cm diameter, showing (left to right) Sc amount per  $120^\circ$  voxel, neutron flux gradient variations in neutron diffusion coefficient and neutron diffusion length; the band widths indicate the theoretical boundaries of these parameters.<sup>(50)</sup>

## 7 SENSITIVITY

Sensitivity is defined as the gradient of the response curve: i.e., the change in instrument response that corresponds to a change in analyte concentration. This definition translates in INAA into the net peak area as a function of the analyte mass. Larger peak areas at a given sample mass can be obtained by the following:

- higher neutron fluxes and longer irradiation times
- more efficient detectors
- larger sample masses.

Higher neutron fluxes and longer irradiation times are often not easily attainable, as the first is limited by reactor design, whereas longer irradiation times only have a positive effect on the sensitivity for radionuclides with very long half-lives.

Absolute photopeak efficiencies of detectors of different sizes and for different geometries are given in Table 7, and a comparison of the absolute efficiencies of a regular 17% coaxial and one of the largest well-type detectors reported in the literature<sup>(51,52)</sup> is given in Figure 12. It should be noted that the use of Compton suppression shields does not result in an increase in sensitivity – as often erroneously suggested; after all, the signal resulting from the induced radioactivity does not increase and sometimes even decreases due to summing-out effects or larger sample-detector distances. Compton suppression systems find their advantage in a decrease in uncertainty of measurement due to decrease of the background under a peak.

Large sample masses can compensate for low neutron fluxes. As the limiting factor in NAA is merely the maximum acceptable induced radioactivity upon

**Table 7** Absolute photopeak efficiencies at some photon energies for 3 detector types and different geometries<sup>(51,52)</sup>

Absolute photopeak efficiency (%)		1332 keV	750 keV	500 keV	250 keV
20%	0 cm	1.5	2.5	3.2	5
	5 cm	0.22	0.35	0.5	1
100%	0 cm	7.5	10	12	16
	5 cm	1	1.4	1.7	2.4
125 cm <sup>3</sup>	Well	5	9	13	25

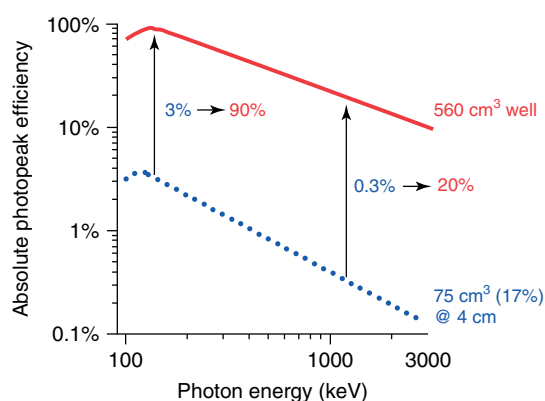


**Figure 12** Schematic absolute full energy photopeak efficiency curves for a regular coaxial Ge detector (17% relative efficiency) and a very large well-type detector.

counting, a comparison has been made with normal INAA in which a hypothetical 200-mg sample is irradiated for a given time at a neutron flux of  $10^{13} \text{ cm}^{-2} \text{ s}^{-1}$ . Assuming a certain neutron fluence rate and a cylindrical sample of similar length and diameter, and an average density of  $0.5 \text{ g cm}^{-3}$ , a first estimate can be made of the minimum

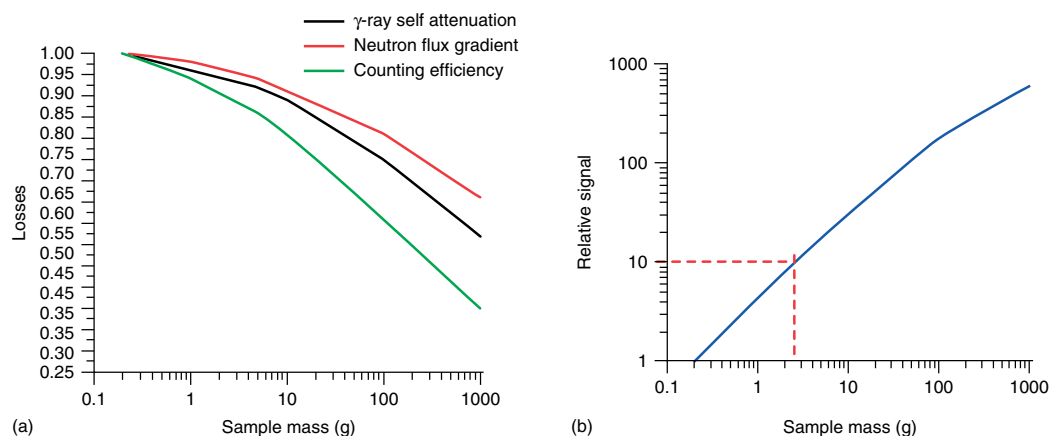


**Figure 13** (a) Losses due to neutron and  $\gamma$ -ray self-shielding and enlarged source-to-detector distance, compared to an analysis of a 200-mg powdered siliceous sample and (b) net gain in signal at increased sample masses.

**Table 8** Indication of minimum sample mass at a given neutron fluence rate to attain similar induced radioactivity as a 200-mg sample, irradiated at  $10^{13} \text{ cm}^{-2} \text{ s}^{-1}$

Neutron fluence rate ( $\text{cm}^{-2} \text{ s}^{-1}$ )	Sample size ( $L, D$ ) (cm)	Sample mass (g)
$2.10^{12}$ – $2.10^{11}$	1–2	1–10
$2.10^{11}$ – $2.10^{10}$	2–4	10–100
$2.10^{10}$ – $2.10^9$	4–7	100–1000
$<2.10^9$	$>7$	$>1 \text{ kg}$

mass needed to reach the same sensitivity as for the small sample at a high neutron fluence rate (Table 8).<sup>(35)</sup>

However, these results must be corrected for the losses due to neutron self-shielding and  $\gamma$ -ray self-attenuation, and the fact that the center of voluminous samples, simply for physical reasons, is always positioned further away from the detector than in case of a small sample. In Figure 13 these effects have been combined, and it can be derived that at a given neutron fluence rate a net gain in signal of a factor of 10 can be obtained by increasing the sample mass by a factor of 15 (e.g., from 200 mg to 3 g).

### 7.1 Natural Background

A large sample NAA procedure should start with measurement of the natural radioactivity of the sample, as the corresponding peaks in the  $\gamma$ -ray spectrum should be separately treated later on in the neutron and  $\gamma$ -ray self-attenuation corrections.

## 8 APPLICATIONS

LSNAA has evolved over the years towards a capability for various samples types that otherwise would have

been difficult to analyze. Accordingly, the developments faced many challenges, each one different from the other, and in this process its horizon of application to various fields has increased: e.g., nutritional studies, geology, biology, archaeology, waste analysis, high-purity material characterization, precious samples, and liquid samples, from all walks of life. A few of them are given in the following text.

### 8.1 Materials Difficult to Homogenize: Geological Samples, Ores, and Waste

LSNAA is highly suitable for the analysis of heterogeneous geological material such as rocks, coal (determination of quality), ores, and mineral concentrates. Conveyor belt monitoring of elemental concentrations by PGNA in coal and cement raw materials has led to an increased efficiency of coal-fired power plants and cement factories. It appears that this technique has the required potential to trigger industrial processes and gives reliable results.

Waste material in many cases is considered to contain hazardous substances whose behavior could result in their entry into biosphere through the atmosphere or ground water. Therefore, appropriate classification of the waste material is required in order to ensure safe disposal or further treatment and recycling. Construction material, domestic and electronic waste, as well as contaminated sediment and compost material are considered to be highly heterogeneous and therefore elaborate sampling procedures are required if representative sampling of these materials for analysis is needed. LSNAA has been effectively used to analyze large samples of soil,<sup>(53)</sup> electronic waste,<sup>(54,55)</sup> and other materials. These are the materials in which both subsampling and homogenization, steps not required in LSNAA, are very difficult and cost intensive. A typical example is the elemental composition analysis of waste from an incineration plant. This type of

sample cannot be easily homogenized and analyzed by other analytical techniques. However, a 1-kg portion of this waste was analyzed by using the LSNA without homogenization.

### 8.2 Materials That May be Contaminated During Homogenization: High-Purity Materials

LSNA is an extremely useful technique to analyze the metals and alloys for impurities. It is being used to analyze various finished products of alloys (Zircaloy 2, Zircaloy 4, SS-316M (stainless steel), and 1S aluminum) that are used in reactor technology<sup>(56)</sup> and for impurities in high technological materials such as silicon and superalloys.<sup>(3)</sup> The biggest advantage is that information is obtained on the entire specimen, and because of the absence of subsampling, contamination can be minimized.

### 8.3 Materials Difficult to Subsample: Nutritional Studies

LSNA is extremely useful in the determination of major, minor, and trace elements in foodstuff, as large samples can be analyzed without resorting to subsampling. In fact, comparison of the results obtained from subsamples of varying mass gave an indication that a sample of 1 kg of wheat is more representative than small samples in the range of 40–1000 mg.<sup>(57)</sup> It is also feasible to determine trace elements in liquid diets, e.g., juices and milk, by LSNA.

### 8.4 Valuable Material of Irregular Shape

Subsampling of archaeological and cultural heritage objects is generally prohibited, as these objects have to be preserved intact. LSNA has the capability for nondestructive bulk analysis of the whole object. In comparison, other established nondestructive analytical methods, such as XRF or analytical techniques based on charged particle irradiation (PIXE, particle induced X-ray emission, IBA, ion beam analysis), can only analyze superficial layers of the sample and provide limited information over the whole volume of the object of interest.<sup>(58,59)</sup>

The particular advantage of INAA being noninvasive and a true multielemental technique is combined in LSNA with the ability to analyze bulky objects as a whole, without any visual damage to the valuable cultural heritage objects. Art historians, conservators, and museum staff do not generally allow damaging such valuable objects by removing a portion for analytical purposes. However, sometimes only the elemental composition can decisively distinguish whether an object is different from what it appears to be from visual inspection.

### 8.5 Other Applications

Direct analysis of large samples provides a unique opportunity for (the validation of) (sub)sampling studies.

## REFERENCES

1. P. Bode, 'Instrumental and Organizational Aspects of a Neutron Activation Analysis Laboratory', Ph.D. thesis, Delft University of Technology, 1996, ISBN 90-73861-42-X.
2. B. Kratochvil, J.K. Taylor, 'Sampling for Chemical Analysis', *Anal. Chem.*, **54**, 924A (1981).
3. M.I. Verheijke, H.J.J. Jaspers, J.M.G. Hanssen, 'Neutron Activation of Very Pure Silicon Wafers', *J. Radioanal. Nucl. Chem.*, **131**, 197 (1989).
4. IUPAC, 'Terminology in Soil Sampling', *Pure Appl. Chem.*, **77**, 825 (2005).
5. P. Bode, R.M.W. Overwater, 'Trace Element Determination in Very Large Samples: A New Challenge for Neutron Activation Analysis', *J. Radioanal. Nucl. Chem.*, **167**, 169 (1993).
6. R.M.W. Overwater, P. Bode, J.J.M. de Goeij, 'Large-sample Neutron Activation Analysis: Present Status and Prospects', *J. Radioanal. Nucl. Chem.*, **216**, 5 (1997).
7. R. Gwozdz, F. Grass, 'Activation Analysis of Large Samples', *J. Radioanal. Nucl. Chem.*, **244**, 523 (2000).
8. X. Lin, R. Henkelmann, 'Instrumental Neutron Activation Analysis of Large Samples: A Pilot Experiment', *J. Radioanal. Nucl. Chem.*, **251**, 197 (2002).
9. R.M.W. Overwater, 'The Physics of Big Sample Instrumental Neutron Activation Analysis', PhD thesis, Delft University of Technology, 1994.
10. C.G. Clayton, A.M. Hassan, M.R. Wormald, 'Multi-element Analysis of Coal During Borehole Logging by Measurement of Prompt  $\gamma$ -Rays from Thermal Neutron Capture', *Int. J. Appl. Radiat. Isot.*, **34**, 83 (1983).
11. G. Vourvopoulos, 'Industrial on Line Bulk Analysis Using Nuclear Techniques', *Nucl. Instrum. Methods*, **B56**, 917 (1991).
12. D.M. Franklin, R. Armstrong, D.R. Chettle, M.C. Scott, 'An Improved in vivo Neutron Activation System for Measuring Kidney Cadmium', *Phys. Med. Biol.*, **35**, 1397 (1990).
13. C.S. Lim, B.D. Sowerby, 'On Line Bulk Elemental Analysis in the Resource Industries Using Neutron-gamma Techniques', *J. Radioanal. Nucl. Chem.*, **264**, 15 (2005).
14. R. Doczi, M.A. Ali, M. Favez-Hassan, J. Csikai, 'Determination of Hydrogen Content in Bulk Samples Using Neutron Activation Analysis', *Appl. Radiat. Isot.*, **63**, 137 (2005).

15. P.A. Beeley, R.G. Garrett, 'Neutron Activation Analysis of Multiple Large Geological Samples by in-pool Irradiation Using a Slowpoke-2 Reactor', *J. Radioanal. Nucl. Chem.*, **167**, 177 (1993).
16. P. Bode, R.M.W. Overwater, J.J.M. de Goeij, 'Large Sample Neutron Activation Analysis: Status and Prospects', *J. Radioanal. Nucl. Chem.*, **216**, 5 (1997).
17. R. Gwozdz, H.J. Hansen, K.L. Rasmussen, H. Kunzendorf, 'Instrumental Neutron Activation Analysis of Samples with Masses from Micrograms to Hectograms', *J. Radioanal. Nucl. Chem.*, **167**, 161 (1993).
18. J.I. Kim, H. Staerk, J. Fiedler, 'A Method of Long-time Irradiation of a Voluminous Liquid Sample in a Reactor Neutron Flux for Activation Analysis of Water', *Nucl. Instrum. Methods*, **177**, 557 (1980).
19. A.G.C. Nair, R. Acharya, K. Sudarshan, S. Gangotra, A.V.R. Reddy, S.B. Manohar, A. Goswami, 'Development of an Internal Monostandard INAA Method Based on in-situ Detection Efficiency for Analysis of Large and Non-standard Geometry Samples', *Anal. Chem.*, **75**, 4868 (2003).
20. F. Tzika, I. Stamatelatos, J. Kalef-Ezra, 'Neutron Activation Analysis of Large Volume Samples: the Influence of Inhomogeneity', *J. Radioanal. Nucl. Chem.*, **271**, 233 (2007).
21. M. Borsaru, R.J. Holmes, P.J. Mathew, 'Bulk Analysis Using Nuclear Techniques', *Int. J. Appl. Radiat. Isot.*, **34**, 397 (1983).
22. M.R. Wormald, C.G. Clayton, 'In-situ Analysis of Coal by Measurement of Neutron-induced Prompt Gamma-rays', *Int. J. Appl. Radiat. Isot.*, **34**, 71–82 (1983).
23. A.T. Farsoni, S.A. Miresghi, 'Design and Evaluation of a TNA Explosive-detection System to Screen Carry-on luggage', *J. Radioanal. Nucl. Chem.*, **248**, 695 (2001).
24. K. Sueiki, K. Kobayashi, W. Sato, H. Nakahara, T. Tomizawa, 'Non Destructive Determination of Major Elements in Large Sample by Prompt Gamma Ray Neutron Activation Analysis', *Anal. Chem.*, **68**, 2203 (1996).
25. K. Sueki, Y. Oura, W. Sato, H. Nakahara, T. Tomizawa, 'Analysis of Archaeological Samples by the Internal Monostandard Method of PGAA', *J. Radioanal. Nucl. Chem.*, **234**, 27 (1998).
26. I.H. Degenaar, M. Blaauw, 'The Neutron Energy Distribution to Use in Monte Carlo Modeling of Neutron Capture in Thermal Neutron Beams', *Nucl. Instrum. Methods*, **B 207**, 131 (2003).
27. J.H. Holloway, H. Akkurt, 'The Fixed Point Formulation for Large Sample PGNAA', *Nucl. Instrum. Methods*, **A522**, 529 (2004).
28. I.H. Degenaar, 'Towards a Methodology for Large Sample Prompt Gamma Neutron Activation Analysis', Ph.D. thesis, Delft University of Technology, 2004, ISBN 90-407-2509-8.
29. W. Gerner, S. Alber, A. Berger, O. Haase, G. Manse, C. Segebade, 'BEAMGAA A Chance for High Precision Analysis of Big Samples', *J. Radioanal. Nucl. Chem.*, **263**, 791 (2005).
30. R. Gwozdz, 'Instrumental Neutron Activation Analysis of Samples with Volumes from 2 to 350 mL', *J. Radioanal. Nucl. Chem.*, **271**, 751 (2007).
31. S.S. Nargolwalla, E.P. Przybylowicz, *Activation Analysis with Neutron Generators*, John Wiley & Sons, New York, 1973.
32. K.G. Broadhead, D.E. Shanks, 'The Application of 2.8 MeV (D,D) Neutrons to Activation Analysis', *Int. J. Appl. Radiat. Isot.*, **18**, 279 (1967).
33. C.J. Evans, S.J.S. Ryde, D.A. Hancock, F. Al-Agel, 'Monte Carlo Simulation of Prompt Gamma Neutron Activation Analysis Using MCNP Code', *Int. J. Appl. Radiat. Isot.*, **49**, 541 (1998).
34. S.A. Natto, D.G. Lewis, S.J.S. Ryde, 'Benchmarking the MCNP Code for Monte Carlo Modeling of an in vivo Neutron Activation Analysis System', *Int. J. Appl. Radiat. Isot.*, **49**, 545 (1998).
35. 'Large Sample NAA Using Low Flux Irradiation Facilities', Report of a Technical Meeting, IAEA, Vienna, Austria, 7–11 November 2005.
36. R. Khelifi, Z. Idiri, P. Bode, A. Amokrane, 'Flux Calculation in LSNAA Using an Am-Be Source', *J. Radioanal. Nucl. Chem.*, **274**, 639 (2007).
37. R. Gwozdz, F. Grass, 'Application of a Radial Geometry for Counting Samples of Mass 10g, to 300g with a Ge-detector', *Environmental Radiochemical Analysis*, Special Publication No. 234, (G.W.A. Newton, Editor), Royal Society of Chemistry, Cambridge, UK, 289 1999.
38. H.W. Baas, M. Blaauw, P. Bode, J.J.M. de Goeij, 'Collimated Scanning Toward 3D-INAA of Inhomogeneous Large Samples', *Fresenius J. Anal. Chem.*, **363**, 753 (1999).
39. G.P. Westphal, 'On the Performance of Loss-Free Counting – A Method for Real-time Compensation of Dead-Time and Pileup Losses in Nuclear Pulse Spectroscopy', *Nucl. Instrum. Methods*, **163**, 189 (1979).
40. F. Girardi, G. Guzzi, J. Pauly, 'Reactor Neutron Activation Analysis by the Single Comparator Method', *Anal. Chem.*, **37**, 1085 (1965).
41. A. Simonits, F. de Corte, J. Hoste, 'Single Comparator Methods in Reactor Neutron Activation Analysis', *J. Radioanal. Chem.*, **24**, 31 (1975).
42. R.M.W. Overwater, J.E. Hoogenboom, 'Accounting for the Thermal Neutron Flux Depression in Voluminous Samples for Instrumental Neutron Activation Analysis', *Nucl. Sci. Eng.*, **117**, 141 (1994).
43. N.S. Shakir, R.E. Jervis, 'Correction Factors Required for Quantitative Large Volume Neutron Activation Analysis', *J. Radioanal. Nucl. Chem.*, **248**, 61 (2001).

44. K. Sudarshan, R. Tripathi, A.G.C. Nair, R. Acharya, A.V.R. Reddy, A. Goswami, 'A Simple Method for Correcting the Neutron Self-shielding Effect of Matrix and Improving the Analytical Response in PGNAA', *Anal. Chim. Acta*, **549**, 205 (2005).
45. R.M.W. Overwater, P. Bode, J.J.M. de Goeij, 'Gamma-ray Spectroscopy of Voluminous Sources: Corrections for Source Geometry and Self-attenuation', *Nucl. Instrum. Methods*, **A324**, 209 (1993).
46. R.M.W. Overwater, P. Bode, 'Computer Simulations of the Effects of Inhomogeneities on the Accuracy of Large Sample INAA', *Int. J. Appl. Radiat. Isot.*, **49**, 967 (1998).
47. H.W. Baas, 'Neutron Activation Analysis of Inhomogeneous Large Samples – An Explorative Study', Ph.D. Dissertation, Delft University of Technology, 2004.
48. P. Bode, E.A. De Nadai Fernandes, R.R. Greenberg, 'Metrology for Chemical Measurements: Purism, Pragmatism and the Position of INAA', *J. Radioanal. Nucl. Chem.*, **245**, 109 (2000).
49. R.M. Lindstrom, R. Zeisler, R.R. Greenberg, 'Accuracy and Uncertainty in Radioactivity Measurement for INAA', *J. Radioanal. Nucl. Chem.*, **271**, 311 (2007).
50. P. Bode, 'Quality Control in Large Sample Analysis', *J. Radioanal. Nucl. Chem.*, **271**, 333 (2007).
51. P. Bode, 'Detectors and Detection Limits in INAA. I. General Theoretical Relationships Between Detector Specifications and Detection Limits', *J. Radioanal. Nucl. Chem.*, **222**, 117 (1997).
52. P. Bode, 'Detectors and Detection Limits in INAA. II. Calculated and Observed Improvements in Detection Limits with Large Ge-detectors, Well-type Ge-detectors and Anti-Compton Spectrometers', *J. Radioanal. Nucl. Chem.*, **222**, 127 (1997).
53. M. Blaauw, H.W. Baas, M. Donze, 'Height-resolved Large-sample INAA of a 1 m long, 13 cm diameter Ditch-bottom Sample', *Nucl. Instrum. Methods*, **A505**, 512 (2003).
54. R.M.W. Overwater, P. Bode, J.J.M. de Goeij, J.E. Hoogenboom, 'Feasibility of Elemental Analysis of Kilogram-Size Samples by Instrumental Neutron Activation Analysis', *Anal. Chem.*, **68**, 341 (1996).
55. C. Segebade, P. Bode, W. Gorner, 'The Problem of Large Samples: An Activation Analysis Study of Electronic Waste Material', *J. Radioanal. Nucl. Chem.*, **271**, 261 (2007).
56. R. Acharya, A.G.C. Nair, A.V.R. Reddy, A. Goswami, 'Standard-less Analysis of Zircaloy Clad Samples by an Instrumental Neutron Activation Method', *J. Nucl. Mater.*, **326**, 80 (2004).
57. R. Acharya, A.G.C. Nair, K. Sudarshan, A.V.R. Reddy, A. Goswami, 'Development and Applications of the  $k_0$ -based Internal Mono Standard INAA Method', *Appl. Radiat. Isot.*, **65**, 164 (2007).
58. K. Janssens, R. van Grieken (eds.), *Comprehensive Analytical Chemistry XLII: Non-destructive microanalysis of cultural heritage materials*, Elsevier, 2005.
59. IAEA STI/DOC/010/416, 'Nuclear Analytical Techniques in Archaeological Investigations', Vienna, 2003.